

Thermal melting of density waves on the square lattice

Adrian Del Maestro and Subir Sachdev

Department of Physics, Yale University, P.O. Box 208120, New Haven, CT 06520-8120, USA

(Dated: January 17, 2014)

We present the theory of the effect of thermal fluctuations on commensurate $p \times p$ density wave ordering on the square lattice ($p \geq 3$, integer). For the case in which this order is lost by a second order transition, we argue that the adjacent state is generically an incommensurate striped state, with commensurate p -periodic long range order along one direction, and incommensurate quasi-long-range order along the orthogonal direction. We also present the routes by which the fully disordered high temperature state can be reached. For $p = 4$, and at special commensurate densities, the 4×4 commensurate state can melt directly into the disordered state via a self-dual critical point with non-universal exponents.

I. INTRODUCTION

A variety of remarkable recent low temperature scanning tunneling microscopy (STM) observations have revealed periodic modulations in the local density of states of the cuprate superconductors^{1,2,3,4}. Notably, the observations of Hanaguri *et al*³ $\text{Ca}_{2-x}\text{Na}_x\text{CuO}_2\text{Cl}_2$ clearly show that the modulations have a commensurate period of 4 lattice spacings along both directions of the underlying square lattice (4×4 ordering). Closely related, but not identical, modulations have been observed in higher temperature STM⁵, and in neutron scattering^{6,7,8,9} observations. The differences between the various experiments relate (*i*) to the period of the ordering, which is incommensurate in Ref. 5, and (*ii*) to whether the ordering extends along one or both of the x and y axes—neutron scattering experiments are more easily explained by anisotropic ordering along one of the axes directions^{10,11,12}. An important open question is whether these differences reflect a fundamental distinction in the underlying electronic structure of the cuprates, or they can be explained by the differing experimental parameters of temperature and carrier concentration.

This paper will begin with the assumption that at very low T , for a small range of carrier densities, and in a sufficiently clean sample, the system has perfect 4×4 density wave order (and, more generally, $p \times p$ order with $p \geq 3$, integer). We will then present a general phenomenological theory of the effect of thermal fluctuations on such an ordered state, describing the phases that appear at higher T and for a wide range of carrier concentration. Because we focus exclusively on thermal fluctuations, our results are quite general and independent of the precise microscopic nature of the density wave ordering; in particular, the ordering could be a site charge density wave, or a modulation in exchange or pairing energies due to valence bond solid order. Our results depend only on the fact that spin-singlet observables acquire a periodic modulation at low T , and follow completely from the symmetry properties of such states. The thermal fluctuations of such an ordered state can, and will, be described by a purely classical theory of the density wave order parameters.

There is a actually large early literature on the melting of a variety to two-dimensional solids on different substrates, and on the commensurate-incommensurate transition^{13,14,15,16,17,18,19,20}. However, most of this work considered the case of the triangular solid on substrates with six-fold symmetry, or the commensurate-incommensurate transition on anisotropic solids. The particular case of interest here, a square lattice substrate and isotropic $p \times p$ ordering, appears not to have been considered previously. We will therefore present an extension of this earlier theory to the situation appropriate for the cuprate superconductors. As we will show below, our results have a number of novel features not found in the cases studied earlier.

We will begin in Section II by defining the order parameters of the commensurate $p \times p$ solid on the square lattice. Symmetry considerations then allow us to obtain a phenomenological free energy density controlling thermal fluctuations of the order parameter, and a corresponding mean field phase diagram shown in Fig. 1. At this stage, this phase diagram contains 3 phases whose characteristics we summarize below:

(A) **Commensurate solid:** This is the ground state with long-range density wave order with period p along both the x and y axes.

(B) **Incommensurate, floating solid:** In mean field theory, this phase has density waves with the same incommensurate period along both the x and y directions. This order is only quasi-long-range *i.e.* density wave correlations decay with a power-law at long distances.

(C) **Liquid:** This is the high temperature phase in which all density wave correlations decay exponentially with distance.

The remainder of the paper will consider fluctuation corrections to this mean field phase diagram.

In mean field theory, the transition between phases A and B is first order, with a jump in the period of the density wave from a commensurate to an incommensurate value. We know from previous work on anisotropic phases^{15,17,18,19} that such commensurate-incommensurate transitions are driven by the proliferation of domain walls, and we consider the domain wall theory for such a transition in Section III. In our case there are two sets of domain walls, running predomi-

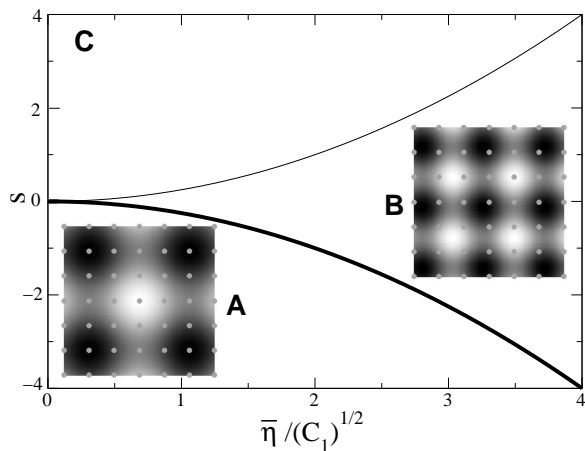


FIG. 1: Mean field phase diagram of the free energy \mathcal{F}_Φ in Eq. (2.4). Although all parameters in \mathcal{F}_Φ are functions of both temperature and carrier concentration, the vertical axis above, s , is primarily a function of temperature. The horizontal axis is tuned by $\bar{\eta}$, which is mainly a measure of carrier concentration away from the commensurate value appropriate to the $p \times p$ ordered state. There are three stable mean field phases separated by a first order transition (thick line), a second order transition (solid line), and a second-order critical point at $s = \bar{\eta} = 0$. The phases A, B, C, are described in the text. For phases A and B we show a schematic of the density modulation $\delta\rho(\mathbf{r})$ for the special case $p = 4$, with the points representing the underlying lattice. Upon including fluctuations, the transition between phases A and B can become second-order; in this situation the phase adjacent to phase A is a new phase B_S , the incommensurate striped phase. The phase B_S preempts a portion (or all) of phase B. See Fig 4 for the fluctuation-corrected phase diagram of phases A and B.

nantly in the x and y directions, and a key parameter will be the intersection energy, f_I , of these domain walls. If $f_I < 0$, then the mean field prediction of a first order transition to an isotropic floating solid is maintained. However, for the case of a positive intersection energy ($f_I > 0$), we will demonstrate that there is a second order transition to an anisotropic, incommensurate “striped” state, which we denote B_S . The B_S state has commensurate long range order with a period of p lattice along one axis, and incommensurate quasi-long-range order along the orthogonal axis. Because B_S has long-range order only along one direction, it may also be labelled a ‘smectic’^{21,22}; however the presence of the underlying lattice makes its fluctuations quite different from a conventional smectic liquid crystal. The striped solid B_S will replace a portion of phase B, so that B_S covers at least the entire second-order phase boundary to phase A (see Fig 4). The remainder of phase B could remain an isotropic floating solid, or it could be anisotropic in its entirety.

Section IV will consider the transitions from the incommensurate states in phase B to the disordered liquid C. Two distinct scenarios are possible, depending upon

the whether the transition takes place from an isotropic floating solid B, or from the anisotropic solid (B_S) which has incommensurate order along only one axis. In either case, the transition is driven by the unbinding of dislocations^{13,14}, and the complete theory for such transitions will be presented.

Finally, Section V will present the theory of the direct transition from the commensurate $p \times p$ solid A to the liquid state C. From Fig. 1 it appears that such a transition is only possible at special commensurate values of the density. For the physically relevant case of $p = 4$ we will find that a direct second order transition is possible. It is described by a self-dual theory with continuously varying exponents, and is a generalization of the theory found in Ref. 23 for the XY model.

II. ORDER PARAMETERS AND MEAN FIELD THEORY

As noted in Section I, all phases and transitions examined here are associated with the order of a generic ‘density’, which could be any observable invariant under spin rotations and time reversal. We represent this density by $\delta\rho(\mathbf{r})$. At sufficiently low temperatures, in weak disorder, and for some range of carrier concentration, we assume that this density prefers to order with a period of p lattice spacings ($p = 4$ is the case of interest for the cuprates). We can therefore write

$$\delta\rho(\mathbf{r}) = \text{Re} [\Phi_x e^{i\mathbf{K}_x \cdot \mathbf{r}}] + \text{Re} [\Phi_y e^{i\mathbf{K}_y \cdot \mathbf{r}}], \quad (2.1)$$

where $\mathbf{K}_x = (2\pi/a)(1/p, 0)$, $\mathbf{K}_y = (2\pi/a)(0, 1/p)$, and $\Phi_{x,y}$ are complex order parameters which vary slowly on the scale of a lattice spacing.

We now want to write down the most general free energy for $\Phi_{x,y}$ consistent with the symmetries of the underlying lattice. Among these are $T_{x,y}$ which translate by a lattice spacing in the x, y directions, and $I_{x,y}$ which reflect the x, y axes. These operations lead to

$$\begin{aligned} T_x &: \Phi_x \rightarrow \Phi_x e^{2i\pi/p} ; \Phi_y \rightarrow \Phi_y \\ T_y &: \Phi_x \rightarrow \Phi_x ; \Phi_y \rightarrow \Phi_y e^{2i\pi/p} \\ I_x &: \Phi_x \rightarrow \Phi_x^* ; \Phi_y \rightarrow \Phi_y \\ I_y &: \Phi_x \rightarrow \Phi_x ; \Phi_y \rightarrow \Phi_y^*. \end{aligned} \quad (2.2)$$

We will also assume the symmetry of rotations by 90 degrees, R , under which

$$R : \Phi_x \rightarrow \Phi_y ; \Phi_y \rightarrow \Phi_x^*. \quad (2.3)$$

This symmetry is absent in some of the cuprate compounds (most notably, in YBCO), and it is not difficult to extend our considerations to include this case.

We can now write down the most general free energy density, expanded in powers of $\Phi_{x,y}$ and its gradients, consistent with the symmetries in Eqs. (2.2) and (2.3)

(see also Refs. 24 and 25). This is

$$\begin{aligned} \mathcal{F}_\Phi = & \int d^2r \left[C_1 \left(|\partial_x \Phi_x|^2 + |\partial_y \Phi_y|^2 \right) \right. \\ & + C_2 \left(|\partial_y \Phi_x|^2 + |\partial_x \Phi_y|^2 \right) \\ & + i\bar{\eta} \left(\Phi_x^* \partial_x \Phi_x + \Phi_y^* \partial_y \Phi_y \right) \\ & + s \left(|\Phi_x|^2 + |\Phi_y|^2 \right) + \frac{u}{2} \left(|\Phi_x|^2 + |\Phi_y|^2 \right)^2 \\ & \left. + v |\Phi_x|^2 |\Phi_y|^2 + w \Phi_x^p + \text{c.c.} + w \Phi_y^p + \text{c.c.} \right]. \quad (2.4) \end{aligned}$$

Here s is a parameter which we will tune to drive the transition; it is assumed to contain the primary dependence on temperature, and will also have some dependence on carrier density.

The term proportional to $\bar{\eta}$ is allowed by the symmetries. It indicates that at sufficiently high temperature, the density correlations are generically *incommensurate*. This incommensurability is a consequence of the values of the domain wall energies between the p commensurate ordered states^{16,20}: a domain wall between state 1 and state 2 (say) will generally have a different energy than a domain wall between state 1 and state p . In other words, if we represent the p states along one direction by a p state clock model, then the interactions of the clock model are ‘chiral’.¹⁶

The sign of the parameter v implies a preference for either isotropic order ($v < 0$ prefers both $\langle \Phi_x \rangle$ and $\langle \Phi_y \rangle$ non-zero), or anisotropic order ($v > 0$ prefers only one of $\langle \Phi_x \rangle$ or $\langle \Phi_y \rangle$ non-zero). We will assume throughout this paper that $v < 0$, so that $\langle \Phi_x \rangle$ and $\langle \Phi_y \rangle$ are both non-zero at sufficiently low temperatures. Nevertheless, we will find that thermal fluctuations can induce an anisotropic striped state over an intermediate temperature range.

The complex parameter w accounts for the commensurability lock-in energy. It ensures that at sufficiently low temperatures (specifically, for s sufficiently negative), the order has a commensurate period of p lattice spacings. For $v < 0$ (assumed throughout), the ordering will be $p \times p$. The phase of w controls the phase of this ordering (‘site-centered’ or ‘bond-centered’). None of our results will be sensitive to this phase, and will apply equally to all of them.

A. Mean field theory

Now we present the results of a simple mean field minimization of \mathcal{F}_Φ , leading to the phase diagram in Fig. 1. As described in the introduction we find three distinct phases. The low temperature ground state, labelled by A has long range density wave order with period p characterized by

$$\Phi_x = \Phi_y \propto e^{i\theta(p)} \quad (2.5)$$

where $\theta(p) = (2n + 1)\pi/p$ if the phase is bond-centered and $\theta(p) = 2n\pi/p$ if the phase is site-centered with $n = 0, 1, \dots, p-1$. The inset in Fig. 1 A shows the locked in solid for the special case of a bond-centered phase with $p = 4$ where the positions of the underlying atoms are indicated by the light gray circles. This commensurate phase has a first order transition described by the line

$$s = - \left(\frac{\sqrt{2u+v-pw}}{\sqrt{2u+v} - \sqrt{2u+v-pw}} \right) \frac{\bar{\eta}^2}{4C_1} \quad (2.6)$$

to B which has incommensurate or floating density wave order characterized by

$$\Phi_x \propto e^{i(\bar{\eta}/2C_1)x} \quad ; \quad \Phi_y \propto e^{i(\bar{\eta}/2C_1)y}. \quad (2.7)$$

The magnitude of both Φ_x and Φ_y are equal and they have the same incommensurate period along perpendicular directions. For the special case of $p = 4$ the floating state is shown as an inset in Fig. 1 B. The floating solid can melt via a second order phase transition defined by the line

$$s = \frac{\bar{\eta}^2}{4C_1} \quad (2.8)$$

to a fully disordered state C with $\Phi_x = \Phi_y = 0$. Finally, there is a tri-critical point for $s = \bar{\eta} = 0$ where the commensurate solid A can melt directly to the liquid phase C.

III. DOMAIN WALL THEORY OF THE COMMENSURATE-INCOMMENSURATE TRANSITION

In Section II A we found a mean-field first order transition between the commensurate $p \times p$ solid A and the incommensurate, isotropic floating solid B. This section will examine fluctuations near this transition more carefully. We will find that the transition can actually be second order under suitable conditions, and the second-order order transition is to an anisotropic, striped state with commensurate p period order along one direction, and incommensurate order along the orthogonal direction.

For our study of the initial melting of the commensurate ordered state, we will assume that dislocations can be ignored. The effect of dislocations will be considered in Section IV, and we will then verify the self-consistency of this assumption. Instead, the primary actors will be domain walls between the commensurate states, as is also the case in previous theories¹⁵ of the commensurate-incommensurate transition in anisotropic systems.

In the absence of dislocations, we can focus on globally defined single-valued angular variables $\theta_{x,y}$ with

$$\Phi_x \propto e^{i\theta_x} \quad ; \quad \Phi_y \propto e^{i\theta_y}. \quad (3.1)$$

Note that the values of $\theta_{x,y}$ span over all real numbers, and not just modulo 2π . However, periodic boundary

conditions need only be satisfied modulo 2π . In the naïve continuum limit, the free energy for $\theta_{x,y}$ can be expanded in powers of the local “strains” $\nabla_{\mathbf{r}}\theta_{x,y}$:

$$\begin{aligned} \mathcal{F}_\theta = & \int d^2r \left[\frac{K_1}{2} [(\partial_x\theta_x)^2 + (\partial_y\theta_y)^2] \right. \\ & + \frac{K_2}{2} [(\partial_x\theta_y)^2 + (\partial_y\theta_x)^2] + K_3(\partial_x\theta_y)(\partial_y\theta_x) \\ & + K_4(\partial_x\theta_x)(\partial_y\theta_y) - \eta[\partial_x\theta_x + \partial_y\theta_y] \\ & \left. - h[\cos(p\theta_x) + \cos(p\theta_y)] - \dots \right]. \end{aligned} \quad (3.2)$$

All terms above are, in principle, obtained from those in Eq. (2.4), but now we have retained terms up to second order in spatial gradients. Now, the incommensuration is induced by the total derivative terms proportional to η : these are non-zero because the angular fields can accumulate an integer multiple of 2π even under periodic boundary conditions. Similarly, we do not have the freedom to integrate by parts, and so combine the terms proportional to K_3 and K_4 . The commensurability energy is now imposed by the p -fold field h_p .

We will begin in Section III A by describing the mean-field structure of the domain wall (or ‘soliton’) excitations of \mathcal{F}_θ . Then, in Section III B we will present the theory of the commensurate-incommensurate transition driven by the proliferation of these domain walls. Section III C will address the nature of density fluctuations within the incommensurate phases: we will estimate the elastic constants of these phases using the domain wall theory of Section III B.

A. Energetics of domain walls

Consider starting at low temperatures from a fully ordered two-dimensional crystal. In this state $\theta_x = 2\pi n/p$, $\theta_y = 2\pi n'/p$, where n, n' are integers, at all points in space. We are now interested in the deviations from this perfectly ordered state as measured by the continuum free energy \mathcal{F}_θ in Eq. (3.2).

The simplest deviation is a single line domain wall in which θ_x increases by $2\pi/p$ across the domain wall. For $\eta > 0$ (which we assume, without loss of generality), such a domain wall will preferentially run in the y direction *i.e.* the domain wall has θ_y constant, and θ_x a function of x only. The x dependence of θ_x can be determined by the sine-Gordon saddle point equation

$$K_1\partial_x^2\theta_x(x) = ph \sin[p\theta_x(x)] \quad (3.3)$$

subject to the boundary conditions

$$\theta_x(0) = 0 \quad ; \quad \theta_x(L_x) = \frac{2\pi}{p} \quad (3.4)$$

where L_x is the size of the system in the x -direction. The

solution is a soliton with equation

$$\theta_x(x) = \frac{4}{p} \tan^{-1} \left[e^{p\sqrt{h/K_1}(x-L_x/2)} \right] \quad (3.5)$$

which allows us to determine the value of the domain wall free energy per unit length (excluding the contribution of the η term in \mathcal{F}_I), which we represent by ϵ ,

$$\epsilon = \frac{8}{p} \sqrt{K_1 h}. \quad (3.6)$$

Similarly, there is a corresponding domain wall in θ_y , with identical physical properties.

Now we consider the interesting case with domain walls running in both the x and y directions. These walls will intersect, and we are interested in the nature of the intersection, and of the intersection free energy f_I . We can focus in on a single domain wall crossing by imposing the boundary conditions of Eq. (3.4) in both the x and y directions. For the special case of perfectly straight domain walls, $\theta_x(x, y) = \theta_x(x)$ and $\theta_y(x, y) = \theta_y(y)$, the only interaction term in Eq. (3.2) can be integrated exactly to give

$$f_I = \left(\frac{2\pi}{p} \right)^2 K_4 \quad (3.7)$$

indicating that the sign of the domain wall intersection energy is equal to the sign of K_4 . When the domain walls are not straight, the interaction energy can be found by numerically minimizing \mathcal{F}_θ and evaluating the interaction terms at the ground state field configurations as seen in Fig. 2. For the following discussion we refer to Fig. 2 and it is assumed that all stiffnesses are measured in units of K_1 . For positive values of K_4 and $K_2 = 1.0$ (panels a through c) we observe straight domain walls for $K_3 < K_2$ and only observe deviation when $K_3 \simeq K_2$. In panel d, $K_3 \simeq K_2 < K_4$ and we find that the walls wander quite significantly. Panels a through d all have $K_4 > 0$ and in agreement with our earlier discussion, $f_I > 0$ in all four configurations. Panel e has no interaction terms ($K_3 = K_4 = 0$) and consequently $f_I = 0$. For negative values of K_4 we find that the domain wall intersection energy changes to a negative value. For $|K_3| < K_2$ the walls remain straight (panels f and g) but as $K_3 \simeq K_4 \simeq -K_2$ the intersection energy becomes large and negative and the system attempts to extend the domain wall overlap over a finite region (panel h).

Although we have only presented eight distinct configurations here, all of the K_j parameter space was examined. When the magnitude of K_3 and K_4 are small with respect to K_2 and K_1 we always find configurations with domain walls crossing at right angles where the domain wall intersection energy can be calculated using Eq. (3.7).

B. Proliferation of domain walls

Now we imagine increasing the parameter η so that the total free energy per unit length of a domain wall is

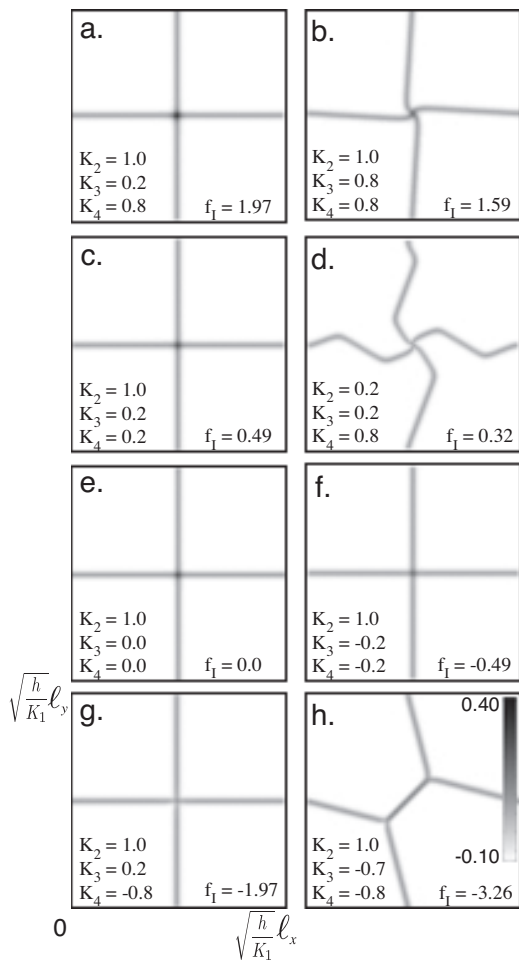


FIG. 2: Eight possible configurations of the free energy density for domain wall crossings depending on the numerical values of K_2 , K_3 and K_4 with $p = 4$. The grey scale plots the size of the local free energy density and all stiffnesses and energies are in units of K_1 . Panels a. through h. show decreasing domain wall intersection energy f_I , and for straight walls, the numerically computed value can be compared with $(\pi^2/4)K_4$.

eventually negative. In such a situation we expect a proliferation of domain walls, leading to the appearance of a floating solid with incommensurate density correlations. This section will discuss the theory of such a transition.

Let the incommensurate state have domain walls in θ_x with an average spacing ℓ_x , and domain walls in θ_y with an average spacing ℓ_y . From the energy per unit length of these domain walls, and their intersection energy, computed in Section III A, there is a clearly a contribution to the free energy per unit area, \mathcal{F}_d , given by (see Fig. 2)

$$\mathcal{F}_d^{(1)}(\ell_x, \ell_y) = \left(\epsilon - \frac{2\pi\eta}{p} \right) \left(\frac{1}{\ell_x} + \frac{1}{\ell_y} \right) + \frac{f_I}{\ell_x \ell_y}. \quad (3.8)$$

However, in addition to the simple energetic contributions in Eq. (3.8), we also have to consider the entropic contribution of the wandering of the domain walls

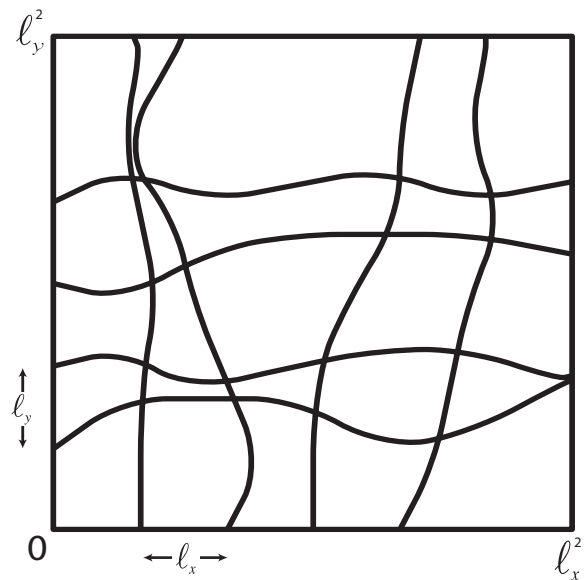


FIG. 3: A net of wandering domain walls constructed using random walkers on a lattice with both hard-core repulsion and restricted phase space. If the domain walls are separated on average by a distance ℓ_x in the x direction and ℓ_y in the y direction, then we observe collisions between domain walls running in the same direction with separation on the order of ℓ_x^2 or ℓ_y^2 ($\ell_x = \ell_y$ here).

(Fig. 3). This can be computed using the elegant free fermion mapping of Pokrovsky and Talapov¹⁵, which applies here (essentially unchanged) separately to the domain walls in each direction. Briefly, the argument runs as follows. Let $u_x(y)$ represent the x co-ordinate of a domain wall in θ_x . Any y dependence in u_x increases the total length of the domain wall, and so leads to a free energy cost

$$\mathcal{F}_w = \frac{1}{2} \epsilon \int dy \left(\frac{du_x}{dy} \right)^2. \quad (3.9)$$

Now the partition function at a temperature T of such domain walls can be mapped onto that for free fermions with a density $1/\ell_x$ and mass ϵ/T . From the ground state energy of such a free fermion system, we then obtain the contribution of the wandering of the domain walls to the free energy density

$$\mathcal{F}_d^{(2)}(\ell_x, \ell_y) = \frac{\pi^2 T^2}{6\epsilon} \left(\frac{1}{\ell_x^3} + \frac{1}{\ell_y^3} \right). \quad (3.10)$$

We are now faced with the simple problem of minimizing the free energy density

$$\mathcal{F}_d(\ell_x, \ell_y) = \mathcal{F}_d^{(1)}(\ell_x, \ell_y) + \mathcal{F}_d^{(2)}(\ell_x, \ell_y) \quad (3.11)$$

as a function of ℓ_x and ℓ_y to determine the nature of the commensurate-incommensurate transition. This simple calculation turns out to have some interesting structure

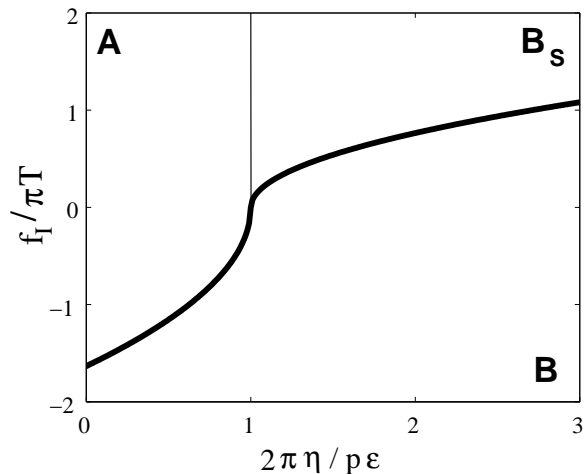


FIG. 4: Phase diagram of the commensurate-incommensurate transition obtained by the minimization of Eq. (3.11) over the values of the mean domain wall spacing ℓ_x and ℓ_y .

which we will now describe. The results of such a minimization are summarized in Fig 4. The nature of the phases appearing here depends upon the sign of the domain wall intersection energy f_I .

For negative f_I corresponding to $K_4 < 0$ in \mathcal{F}_θ , as we increase the value of η the mean field prediction is preserved, and the ground state with long range charge density wave order melts via a first order transition to an isotropic incommensurate floating solid which we labelled as B. This transition occurs when

$$\eta_{AB} = \frac{p\epsilon}{2\pi} \left[1 - \frac{3}{8} \left(\frac{f_I}{\pi T} \right)^2 \right]. \quad (3.12)$$

That is, for $\eta < \eta_{AB}$ the system is commensurate with $1/\ell_x = 1/\ell_y = 0$ but for $\eta > \eta_{AB}$ there is a jump to the isotropic floating state B with domain wall densities

$$\frac{1}{\ell_x} = \frac{1}{\ell_y} = -\frac{f_I \epsilon}{\pi^2 T^2} + \sqrt{\left(\frac{f_I \epsilon}{\pi^2 T^2} \right)^2 - \frac{2\epsilon(\epsilon - 2\pi\eta/p)}{\pi^2 T^2}}. \quad (3.13)$$

If the domain wall intersection energy is positive, implying that collisions are disfavored ($f_I > 0$, $K_4 > 0$), then as we increase the value of η from zero the state remains commensurate with long range order and no domain walls ($1/\ell_x = 1/\ell_y = 0$) until

$$\eta_{AB_S} = \frac{p\epsilon}{2\pi} \quad (3.14)$$

where there is a second order phase transition to a state with (say)

$$\frac{1}{\ell_y} = 0 \quad ; \quad \frac{1}{\ell_x} = \frac{1}{\pi T} \sqrt{2\epsilon \left(\frac{2\pi\eta}{p} - \epsilon \right)} \quad (3.15)$$

which has domain walls running in *either* the x or y direction but not *both*. This anisotropic floating solid or

incommensurate striped state which we label B_S has long range charge density wave order with period p in one direction and quasi long range order with power law decay in the perpendicular direction. Near the second-order transition between A and B_S , insertion of Eq. (3.15) into Eq. (3.11) shows that $\mathcal{F}_d \sim -(\epsilon - 2\pi\eta/p)^{3/2}$.

As η is increased further for $f_I > 0$, the phase B_S persists until

$$\eta_{B_S B} = \frac{p\epsilon}{2\pi} \left[1 + (1.70968 \dots) \left(\frac{f_I}{\pi T} \right)^2 \right] \quad (3.16)$$

where there is a first order transition to the isotropic incommensurate floating solid B with ℓ_x and ℓ_y still given by Eq. (3.13). In fact, the solution in Eq. (3.13) is a local minimum of the free energy for all $\eta > p\epsilon/(2\pi)$. However, its free energy behaves like $\mathcal{F}_d \sim -(\epsilon - 2\pi\eta/p)^2$ upon approaching phase A. Close enough to phase A, this free energy is always larger than the free energy for phase B_S .

Therefore, if the intersection energy for domain walls is positive, the melting of the commensurate solid A always occurs via a second-order transition to the striped anisotropic state B_S .

C. Renormalization of elastic constants in incommensurate phases

Once the domain walls have proliferated in phases B and B_S , the density correlations become incommensurate and appear at wavevectors which are shifted from the commensurate values in Eq. (2.1). We are interested here in the long wavelength ‘‘spinwave’’ density fluctuations about this incommensurate state.

First, let us consider the phase B. Rather than defining the spin-wave variables about the commensurate state as in Eq. (3.1), we now need to look at fluctuations above an incommensurate ordered state. So now we write

$$\Phi_x \propto e^{i2\pi x/(p\ell_x)} e^{i\theta_x} \quad ; \quad \Phi_y \propto e^{i2\pi y/(p\ell_y)} e^{i\theta_y}, \quad (3.17)$$

because the incommensurate ordering wavevectors are $(2\pi/a)(1/p + a/\ell_x, 0)$ and $(2\pi/a)(0, 1/p + a/\ell_y)$. We are interested in the effective action for these $\theta_{x,y}$ on a coarse-grained scale much larger than $\ell_{x,y}$. This action can be deduced by the same symmetry arguments made in Section II. It is not difficult to see that this action in the floating phase B has the same structure as \mathcal{F}_θ in Eq. (3.2), except that now $\eta = h = 0$:

$$\begin{aligned} \mathcal{F}_B = & \int d^2 r \left[\frac{K_1}{2} [(\partial_x \theta_x)^2 + (\partial_y \theta_y)^2] \right. \\ & + \frac{K_2}{2} [(\partial_x \theta_y)^2 + (\partial_y \theta_x)^2] + K_3 (\partial_x \theta_y) (\partial_y \theta_x) \\ & \left. + K_4 (\partial_x \theta_x) (\partial_y \theta_y) \right] \quad (3.18) \end{aligned}$$

For the phase B_S , the θ_y variables (say) are locked at their commensurate value, and so only the θ_x variables will contribute to the spin-wave theory:

$$\mathcal{F}_{B_S} = \int d^2r \left[\frac{K_1}{2} (\partial_x \theta_x)^2 + \frac{K_2}{2} (\partial_y \theta_x)^2 \right] \quad (3.19)$$

An important point is that the stiffnesses K_{1-4} in Eqs. (3.18) and (3.19) be strongly renormalized from the bare values in Eq. (3.2). Following the analysis of Ref. 17, we will now estimate their renormalized values K_{1-4}^R in terms of the parameters appearing in the domain wall free energies in Section III B (the superscript R will be used for clarity only in this subsection).

First, imagine that we impose a uniform compressional strain $\partial_x \theta_x$ on the floating solid. On the average, this will cause the domain walls to move closer to each other, and change the value of ℓ_x to $\ell_x - \delta \ell_x$. Because θ_x changes by $2\pi/p$ across each domain wall, we conclude that $\partial_x \theta_x = (2\pi/p) \delta \ell_x / \ell_x^2$. The change in ℓ_x will cause a change in free energy that can be computed from Eq. (3.11), and so we conclude

$$K_1^R = \frac{p^2 \ell_x^4}{4\pi^2} \frac{\partial^2 \mathcal{F}_d}{\partial \ell_x^2}, \quad (3.20)$$

where the derivative has to be computed at the equilibrium values of ℓ_x, ℓ_y which minimize Eq. (3.11). This determines

$$K_1^R = \frac{p^2 T^2}{4\epsilon \ell_x}, \quad (3.21)$$

in both phases B and B_S . Similarly, we can apply a combined compressional strain in θ_x and θ_y and conclude

$$K_4^R = \frac{p^2 \ell_x^2 \ell_y^2}{4\pi^2} \frac{\partial^2 \mathcal{F}_d}{\partial \ell_x \partial \ell_y}, \quad (3.22)$$

This is non-zero only in the floating phase B, and we obtain

$$K_4^R = \frac{p^2 f_I}{4\pi^2}, \quad \text{phase B only.} \quad (3.23)$$

To determine K_2^R , apply a small uniform shear strain to θ_x by inducing a non-zero $\partial_y \theta_x$. This will move the domain walls in θ_x such that the position of each domain wall obeys $\partial_y u_x = (p \ell_x / (2\pi)) \partial_y \theta_x$. Inserting this into Eq. (3.9), we obtain

$$K_2^R = \frac{\epsilon}{\ell_x} \left(\frac{p \ell_x}{2\pi} \right)^2 = \frac{\epsilon p^2 \ell_x}{4\pi^2}, \quad (3.24)$$

in both phases B and B_S .

Finally, to determine K_3^R we need to apply shear strains to both θ_x and θ_y . Neither of them causes a net change in the density of domain walls, or in the number of intersections between the domain walls. Consequently there is no change to the free energy beyond that already accounted for by K_2^R , and hence

$$K_3^R = 0, \quad (3.25)$$

in both phases B and B_S .

IV. DISLOCATION MEDIATED MELTING OF FLOATING SOLIDS

We will now consider the transition from the isotropic floating solid B and the striped floating solid B_S to the disordered liquid phase C. These transitions are driven by the unbinding of dislocations.

With the parameters of the ‘‘spin-wave’’ theory at hand in Section III C, we can address the energetics of the dislocations. We will derive the effective action for the dislocations in Section IV A and then obtain the renormalization group (RG) flow equations in Section IV B.

A. Dislocation interactions

For the most part, this section will be restricted to a discussion of dislocations in phase B. The simpler case of the anisotropic phase B_S is easily obtained by only including those terms arising from the fluctuations of θ_x .

Dislocations are simply ‘vortices’ in the angular fields $\theta_{x,y}$ under which

$$\begin{aligned} \oint d\mathbf{r} \cdot \nabla_{\mathbf{r}} \theta_x &= 2\pi m_x(\mathbf{r}_v) \\ \oint d\mathbf{r} \cdot \nabla_{\mathbf{r}} \theta_y &= 2\pi m_y(\mathbf{r}_v) \end{aligned} \quad (4.1)$$

where $m_{x,y}$ are integers at the vortex (*i.e.* dislocation) site \mathbf{r}_v , and the integral is over a contour that encloses \mathbf{r}_v . Each dislocation is therefore characterized by a doublet of integers (m_x, m_y) .

To compute the interactions between these vortices, it is useful to define continuum vortex densities by

$$m_i(\mathbf{r}) = \sum_v m(\mathbf{r}_v) \delta(\mathbf{r} - \mathbf{r}_v) \quad (4.2)$$

where $i = x, y$. Then, after transforming to momentum (\mathbf{k}) space, the relation Eq. (4.1) can be written simply as

$$k_i \vartheta_j = k_i \vartheta_j + \frac{2\pi}{k^2} \epsilon_{i\ell} k_\ell m_j \quad (4.3)$$

where ϵ is the antisymmetric tensor, and ϑ_j is an arbitrary smooth angular field which has no vortices. We now insert Eq. (4.3) into the free energy \mathcal{F}_B in Eq. (3.18), and minimize with respect to ϑ_j . The result for the total free energy of the vortices is then

$$\begin{aligned} \mathcal{F}_v &= \int \frac{d^2 k}{4\pi^2} \frac{2\pi^2}{D(k_x, k_y)} \left[|m_x(\mathbf{k})|^2 (k_x^2 K_1 (K_2^2 - K_3^2)) \right. \\ &+ k_y^2 K_2 (K_1^2 - K_4^2) + |m_y(\mathbf{k})|^2 (k_y^2 K_1 (K_2^2 - K_3^2)) \\ &+ k_x^2 K_2 (K_1^2 - K_4^2) + m_x(\mathbf{k}) m_y(-\mathbf{k}) k_x k_y (K_1^2 K_3 \\ &+ K_2^2 K_4 - K_3 K_4 (K_3 + K_4)) \left. \right] \end{aligned} \quad (4.4)$$

where

$$D(k_x, k_y) \equiv K_1 K_2 (k_x^2 + k_y^2)^2 + k_x^2 k_y^2 ((K_1 - K_2)^2 - (K_3 + K_4)^2). \quad (4.5)$$

Note that the values of K_{1-4}^R from Section III C are to be inserted into the expressions above; here, and henceforth, the superscript R has been dropped. The interaction between the vortices is now determined by transforming Eq. (4.4) back to real space. This takes the form

$$\begin{aligned} \mathcal{F}_v = & E_c \sum_v [m_x^2(\mathbf{r}_v) + m_y^2(\mathbf{r}_v)] \\ & + \sum_{v < v'} \left[m_x(\mathbf{r}_v) m_x(\mathbf{r}_{v'}) V(|\mathbf{r}_v - \mathbf{r}_{v'}|, \phi(\mathbf{r}_v - \mathbf{r}_{v'})) \right. \\ & + m_y(\mathbf{r}_v) m_y(\mathbf{r}_{v'}) V(|\mathbf{r}_v - \mathbf{r}_{v'}|, \phi(\mathbf{r}_v - \mathbf{r}_{v'}) + \pi/2) \\ & \left. + m_x(\mathbf{r}_v) m_y(\mathbf{r}_{v'}) W(|\mathbf{r}_v - \mathbf{r}_{v'}|, \phi(\mathbf{r}_v - \mathbf{r}_{v'})) \right] \quad (4.6) \end{aligned}$$

where $\phi(\mathbf{r}) = \arctan(y/x)$ is the angle the vector \mathbf{r} makes with the x axis. We will not need the explicit form of the interaction W in our subsequent analysis, and so we will not specify it explicitly; the interaction V is given by

$$\begin{aligned} V(r, \phi) = & \int_0^\infty \frac{e^{-ka} dk}{k} \int_0^{2\pi} d\varphi \left[e^{ikr \cos(\phi - \varphi)} - 1 \right] \\ & \times \frac{K_1(K_2^2 - K_3^2) \cos^2 \varphi + K_2(K_1^2 - K_4^2) \sin^2 \varphi}{K_1 K_2 + ((K_1 - K_2)^2 - (K_3 + K_4)^2) \sin^2 \varphi \cos^2 \varphi} \\ = & \frac{p^2 T^2}{4\pi^2} \int_0^{2\pi} d\varphi \int_0^\infty \frac{e^{-ka} dk}{k} [\cos(kr \cos(\phi - \varphi)) - 1] \\ & \times \Lambda(\tilde{K}_i, \varphi) \\ \equiv & -\frac{p^2 T^2}{2\pi} \tilde{L}_0 \ln(r/a) + \tilde{V}(\phi) \quad (4.7) \end{aligned}$$

where we have inserted a soft cutoff using the lattice spacing a , and

$$\begin{aligned} \Lambda(\tilde{K}_i, \varphi) & \quad (4.8) \\ = & \frac{\tilde{K}_2 \cos^2 \varphi + \tilde{K}_1 \sin^2 \varphi}{\tilde{K}_1 \tilde{K}_2 + ((\tilde{K}_1 - \tilde{K}_2)^2 - (\tilde{K}_3 + \tilde{K}_4)^2) \sin^2 \varphi \cos^2 \varphi} \end{aligned}$$

is a function of the new couplings \tilde{K}_{1-4} defined by

$$\begin{aligned} \tilde{K}_1 = \frac{p^2 T^2}{4\pi^2} \frac{K_2}{K_2^2 - K_3^2} \quad ; \quad \tilde{K}_2 = \frac{p^2 T^2}{4\pi^2} \frac{K_1}{K_1^2 - K_4^2} \\ \tilde{K}_3 = \frac{p^2 T^2}{4\pi^2} \frac{K_4}{K_1^2 - K_4^2} \quad ; \quad \tilde{K}_4 = \frac{p^2 T^2}{4\pi^2} \frac{K_3}{K_2^2 - K_3^2}. \quad (4.9) \end{aligned}$$

At this point these definitions of the \tilde{K}_{1-4} may be viewed as arbitrary variables, but we will see later in Section V and Appendix B that these are the couplings that appear in a self-dual mapping of the theory \mathcal{F}_θ . Also, from

Appendix B, note that the \tilde{K}_{1-4} couplings appear upon taking the inverse of the matrix of couplings between the strains in \mathcal{F}_B ; consequently, the inverse expressions for the K_{1-4} in terms of the \tilde{K}_{1-4} have exactly the same structure as in Eq. (4.9). The parameters in the last line of Eq. (4.7) are given by

$$\begin{aligned} \tilde{L}_0 & = \int_0^{2\pi} \frac{d\varphi}{2\pi} \Lambda(\tilde{K}_i, \varphi) \quad (4.10) \\ & = \frac{\tilde{K}_1 + \tilde{K}_2}{\sqrt{\tilde{K}_1 \tilde{K}_2 [(\tilde{K}_1 + \tilde{K}_2)^2 - (\tilde{K}_3 + \tilde{K}_4)^2]}} \\ \tilde{V}(\phi) & = -\frac{p^2 T^2}{4\pi^2} \int_0^{2\pi} d\varphi \ln(|\cos(\phi - \varphi)|) \Lambda(\tilde{K}_i, \varphi) \end{aligned}$$

where the calculation of \tilde{L}_0 is described in Appendix A. For $\tilde{K}_3 = \tilde{K}_4 = 0$, $\tilde{V}(\phi)$ can be evaluated in closed form:

$$\tilde{V}(\phi) = \frac{p^2 T^2}{4\pi(\tilde{K}_1 \tilde{K}_2)^{1/2}} \ln \left(\frac{(\tilde{K}_1^{1/2} + \tilde{K}_2^{1/2})^2}{\tilde{K}_1 \sin^2 \phi + \tilde{K}_2 \cos^2 \phi} \right). \quad (4.11)$$

B. Renormalization group flows

With the knowledge of the interactions between the dislocations, the renormalization group equations can be derived by the methods already described in Refs. 13 and 14. We introduce a vortex fugacity, $y = e^{-E_c/T}$ and examine the effect of integrating out pairs of dislocations in an expansion in powers of y . A simple and standard analysis shows that the flow equation for the fugacity is

$$\frac{dy}{d\ell} = \left(2 - \frac{p^2 T}{4\pi} \tilde{L}_0 \right) y. \quad (4.12)$$

The renormalization of the K_i from the vortices can be computed by the method described in Appendix B of Ref. 14. We compute the renormalization of the elastic constants, K_i by determining the contribution of the vortices to a two-point correlation of the strains. Such a procedure leads naturally to flow equations for the ‘inverse’ or ‘dual’ \tilde{K}_i couplings, and we obtain

$$\begin{aligned} \frac{d\tilde{K}_1}{d\ell} & = p^2 y^2 T \int_0^{2\pi} d\phi \cos^2 \phi e^{\tilde{V}(\phi)/T} \\ \frac{d\tilde{K}_2}{d\ell} & = p^2 y^2 T \int_0^{2\pi} d\phi \sin^2 \phi e^{\tilde{V}(\phi)/T} \\ \frac{d\tilde{K}_3}{d\ell} & = 0 \\ \frac{d\tilde{K}_4}{d\ell} & = 0 \quad (4.13) \end{aligned}$$

We can convert these into equations for the K_i and obtain

$$\begin{aligned}\frac{dK_1}{d\ell} &= -\frac{4\pi^2 y^2}{T}(K_1^2 + K_4^2) \int_0^{2\pi} d\phi \sin^2 \phi e^{\tilde{V}(\phi)/T} \\ \frac{dK_2}{d\ell} &= -\frac{4\pi^2 y^2}{T}(K_2^2 + K_3^2) \int_0^{2\pi} d\phi \cos^2 \phi e^{\tilde{V}(\phi)/T} \\ \frac{dK_3}{d\ell} &= -\frac{8\pi^2 y^2}{T} K_2 K_3 \int_0^{2\pi} d\phi \cos^2 \phi e^{\tilde{V}(\phi)/T} \\ \frac{dK_4}{d\ell} &= -\frac{8\pi^2 y^2}{T} K_1 K_4 \int_0^{2\pi} d\phi \sin^2 \phi e^{\tilde{V}(\phi)/T} \quad (4.14)\end{aligned}$$

While complex in appearance, the flow equations Eq. (4.12) and (4.14) predict a melting transition of the floating phase B into the liquid phase C which is in a universality class closely related to that of the Kosterlitz-Thouless (KT) transition. The phase B is stable provided $\tilde{L}_0 > 8\pi/(p^2 T)$. Evaluating \tilde{L}_0 at the values of the K_i^R determined in Section III C, we find that phase B is stable everywhere for $p = 4$ towards an infinitesimal vortex fugacity for the elastic constants in the domain wall theory; this justifies the neglect of dislocations in our study of domain wall proliferation in Section III. The present equations Eq. (4.14) show how phase B will ultimately become unstable to a vortex unbinding transition once the vortex fugacity becomes larger. The flow equations in Eq. (4.14) imply singularities in the elastic constants just before the melting transition which can be computed as in Ref. 26. Some of the universal amplitude ratios here will be different from the KT transition, but all exponents and critical singularities will be as in the KT transition.

The flow equations for the melting of the anisotropic phase B_S can be easily obtained from Eq. (4.14) simply by setting $K_3 = K_4 = 0$. In this case, the values of the elastic constants in Section III C and Eq. (4.10) imply that

$$\tilde{L}_0 = \frac{4\pi^2}{p^2 T^2} (K_1^R K_2^R)^{1/2} = \frac{\pi}{T}. \quad (4.15)$$

The equation for the vortex fugacity Eq. (4.12) implies then that the vortex fugacity flows to zero as long as¹⁷ $p^2 > 8$, which is certainly the case for $p > 3$. Hence the floating phase B_S is also initially stable to dislocation unbinding. At higher temperatures, there can be a dislocation unbinding transition in the Kosterlitz-Thouless universality class. Note that in this sequence of transitions, even after such a transition has occurred from the phase B_S , order has only been lost in x direction, and commensurate long-range order remains in θ_y . So the system is still strongly “striped” and anisotropic. Full isotropy will be restored only after a second set of similar transitions in θ_y , the first to floating incommensurate order in θ_y , and then a dislocation unbinding transition to the liquid phase C.

V. DIRECT MELTING OF THE COMMENSURATE SOLID

As we noted in Section I and Fig 1, it is possible that the low temperature 4×4 commensurate solid can melt directly into the high temperature liquid state. In the theories \mathcal{F}_Φ in Eq. (2.4) and \mathcal{F}_θ in Eq. (3.2), such a transition appears possible at commensurate densities at which $\bar{\eta} = \eta = 0$. So this section will neglect the influence of η and perform a full renormalization group analysis of the theory \mathcal{F}_θ , including both dislocations and the p -fold lock-in field h .

A key property which aids the analysis is a self-duality of the action in which the dislocation fugacity, y , and the lock-in field h are interchanged. The origin of this self-duality is similar to that discussed in Ref. 23, and we present a brief derivation in Appendix B. From this analysis we obtain the the partition function \mathcal{F}_θ , including dislocations, obeys

$$\mathcal{Z}_\theta(K_1, K_2, K_3, K_4, h, y) = \mathcal{Z}_\theta(\tilde{K}_1, \tilde{K}_2, \tilde{K}_3, \tilde{K}_4, y, h), \quad (5.1)$$

where the couplings \tilde{K}_i were defined in Eq. (4.9).

Aided by this duality, we can now immediately deduce the full flow equations for all the elastic constants K_i , the vortex fugacity y and the field h from the results in Section IV B. As always, these equations are valid for small y and h and are

$$\begin{aligned}\frac{dh}{d\ell} &= \left(2 - \frac{p^2 T}{4\pi} L_0\right) h \\ \frac{dy}{d\ell} &= \left(2 - \frac{p^2 T}{4\pi} \tilde{L}_0\right) y \\ \frac{dK_1}{d\ell} &= \int_0^{2\pi} d\phi \left[p^2 h^2 T \cos^2 \phi e^{V(\phi)/T} \right. \\ &\quad \left. - \frac{4\pi^2 y^2}{T} (K_1^2 + K_4^2) \sin^2 \phi e^{\tilde{V}(\phi)/T} \right] \\ \frac{dK_2}{d\ell} &= \int_0^{2\pi} d\phi \left[p^2 h^2 T \sin^2 \phi e^{V(\phi)/T} \right. \\ &\quad \left. - \frac{4\pi^2 y^2}{T} (K_2^2 + K_3^2) \cos^2 \phi e^{\tilde{V}(\phi)/T} \right] \\ \frac{dK_3}{d\ell} &= -\frac{8\pi^2 y^2}{T} K_2 K_3 \int_0^{2\pi} d\phi \cos^2 \phi e^{\tilde{V}(\phi)/T} \\ \frac{dK_4}{d\ell} &= -\frac{8\pi^2 y^2}{T} K_1 K_4 \int_0^{2\pi} d\phi \sin^2 \phi e^{\tilde{V}(\phi)/T} \quad (5.2)\end{aligned}$$

Here L_0 and $V(\phi)$ are defined as in Eq. (4.10), but with direct couplings:

$$\begin{aligned}L_0 &= \int_0^{2\pi} \frac{d\phi}{2\pi} \Lambda(K_i, \phi) \\ V(\phi) &= -\frac{p^2 T^2}{4\pi^2} \int_0^{2\pi} d\varphi \ln(|\cos(\phi - \varphi)|) \Lambda(K_i, \varphi)\end{aligned} \quad (5.3)$$

We will confine our analysis of Eq. (5.2) to the physically important case of $p = 4$. For this case, we first searched for an intermediate phase with power-law correlations: such a phase would obtain if there was a set of values of K_{1-4} for which *both* y and h flowed to zero. As shown in Appendix A, there is no such regime of parameters.

However, the flow equations in Eq. (5.2) do predict a direct second-order transition between the 4×4 commensurate solid A and isotropic liquid C. This transition is described by a manifold of fixed points. In the 6-dimensional space of couplings, there is 2-dimensional manifold of fixed points specified by

$$y = h \ ; \ \frac{K_1 K_2}{T^2} = \frac{4}{\pi^2} \ ; \ K_3 = K_4 = 0. \quad (5.4)$$

In order to describe the flows near this manifold, it is convenient to make a change of variables from y , h , K_1 , and K_2 to

$$K = \frac{\sqrt{K_1 K_2}}{T} - \frac{2}{\pi} \ , \quad \lambda = \sqrt{\frac{K_1}{K_2}} \ . \quad (5.5)$$

In these variables, the fixed point manifold is described by $\alpha = K = K_3 = K_4 = 0$, while the values of λ and β are arbitrary. All physical properties, including the exponents at the second-order critical point, will depend upon the bare values of λ and β . We expanded Eqs. (5.2) to linear order in α , K , K_3 , and K_4 , and after diagonalization of the flow equations, obtained the following renormalization group eigenvalues in this 4-dimensional subspace:

$$\begin{aligned} & 2\pi^2\beta \left(\sqrt{\lambda} + 1/\sqrt{\lambda} \right)^4 \\ & \times \left(1 \pm \left(1 + \frac{4}{\pi^2\beta \left(\sqrt{\lambda} + 1/\sqrt{\lambda} \right)^4} \right)^{1/2} \right), \\ & - 4\pi^2\beta^2 \left(\sqrt{\lambda} + 1/\sqrt{\lambda} \right)^4, \end{aligned} \quad (5.6)$$

where the last eigenvalue is doubly degenerate. It is evident that for all λ , β there are 3 negative eigenvalues and 1 positive eigenvalue. This flow therefore describes a conventional second-order transition, with the correlation length exponent ν equal to the inverse of the positive eigenvalue.

VI. CONCLUSIONS

We have shown that thermal fluctuations on 4×4 ordered state lead generically to a rather rich phase diagram as a function of temperature and carrier concentration. This phase diagram generically must have regions with incommensurate and anisotropic ordering. Thus it

is remains within the realm of possibility that the underlying physics of density wave ordering in all the cuprates is the same, and the distinctions between the experiments are entirely due to their distinct locations in our phase diagram.

For easy reference, we conclude by listing the various routes the 4×4 solid A can melt into the liquid C. The list below is not exhaustive, and omits certain possibilities involving strong first order transitions between unrelated phases.

1. Phase A undergoes a second order Pokrovsky-Talapov¹⁵ (PT) transition to the incommensurate striped phase B_S , as described in Section III B. This is followed by a first order transition into phase B as also described in Section III B and Fig 4. Then phase B undergoes a dislocation mediated melting transition into phase C which is described by Eqs. (4.12) and (4.14). This last transition is in a universality class which is nearly, but not exactly, KT.
2. PT transition from phase A to phase B_S as in 1. Phase B_S then has a KT transition to a striped state which has long range order with period 4 along one direction, and exponentially decaying correlations along the other. This striped set melts into C after a second set of similar transitions: a PT transition into a state with incommensurate quasi-long range order in one direction only, and then finally a KT transition in C.
3. First order transition from A to B as described in Section III B and Fig 4. Then, a transition from B to C as in 2.
4. At special commensurate densities, there is a direct, self-dual, second-order transition from A to C, described in Section V, with continuously varying exponents.

Acknowledgments

We thank E. Fradkin, S. Kivelson, and T. Lubensky for valuable discussions. This research was supported by the National Science Foundation under grant DMR-0098226, and under grants DMR-0210790, PHY-9907949 at the Kavli Institute for Theoretical Physics. S.S. was also supported by the John Simon Guggenheim Memorial Foundation.

APPENDIX A: EVALUATION OF \tilde{L}_0

This appendix will present the derivation of \tilde{L}_0 in Eq. (4.10) and its application to the flow equations presented in Section V. We begin by writing the integral

explicitly as

$$\begin{aligned} \tilde{L}_0 &= \int_0^{2\pi} \frac{d\varphi}{2\pi} \quad (A1) \\ &\times \frac{\tilde{K}_2 \cos^2 \varphi + \tilde{K}_1 \sin^2 \varphi}{\tilde{K}_1 \tilde{K}_2 + [(\tilde{K}_1 - \tilde{K}_2)^2 - (\tilde{K}_3 + \tilde{K}_4)^2] \sin^2 \varphi \cos^2 \varphi} \\ &= \int_0^{2\pi} \frac{d\varphi}{\pi} \left[\frac{\tilde{K}_1 + \tilde{K}_2}{\alpha^+ - \alpha^- \cos^2 2\varphi} + \frac{(\tilde{K}_2 - \tilde{K}_1) \cos 2\varphi}{\alpha^+ - \alpha^- \cos^2 2\varphi} \right] \end{aligned}$$

where

$$\alpha^\pm = (\tilde{K}_1 \pm \tilde{K}_2)^2 - (\tilde{K}_3 + \tilde{K}_4)^2. \quad (A2)$$

The second term in the last line of Eq. (A1) is identically zero and we are left with

$$\begin{aligned} \tilde{L}_0 &= (\tilde{K}_1 + \tilde{K}_2) \int_0^{2\pi} \frac{d\varphi}{\pi} \frac{1}{\alpha^+ - \alpha^- \cos^2 2\varphi} \\ &= 2 \frac{\tilde{K}_1 + \tilde{K}_2}{\sqrt{\alpha^+(\alpha^+ - \alpha^-)}} \\ &= \frac{\tilde{K}_1 + \tilde{K}_2}{\sqrt{\tilde{K}_1 \tilde{K}_2 [(\tilde{K}_1 + \tilde{K}_2)^2 - (\tilde{K}_3 + \tilde{K}_4)^2]}}, \quad (A3) \end{aligned}$$

which can be written in terms of our original coupling constants K_i as

$$\tilde{L}_0 = \frac{4\pi^2}{p^2 T^2} \frac{K_1(K_2^2 - K_3^2) + K_2(K_1^2 - K_4^2)}{\sqrt{K_1 K_2 [(K_1 + K_2)^2 - (K_3 + K_4)^2]}}. \quad (A4)$$

This is not to be confused with L_0 from Eq. (5.2) which is given by

$$L_0 = \frac{K_1 + K_2}{\sqrt{K_1 K_2 [(K_1 + K_2)^2 - (K_3 + K_4)^2]}}. \quad (A5)$$

For the direct transition from A to C (Section V) for $p = 4$ we wish to determine if there is any region close to the manifold of fixed points where both h and y are irrelevant. We do this by expanding Eqs. (A4) and (A5) for small K_3 and K_4 parameterized by

$$K_3 = \delta_3 K_2 \quad ; \quad K_4 = \delta_4 K_1, \quad (A6)$$

where $|\delta_3|$ and $|\delta_4| < 1$ and substituting into the expressions for $dh/d\ell$ and $dy/d\ell$ in Eq. (5.2). Define

$$\beta(h) = \frac{1}{h} \frac{dh}{d\ell} \quad ; \quad \beta(y) = \frac{1}{y} \frac{dy}{d\ell}, \quad (A7)$$

it is then straightforward to show that $\beta(h) \geq 0$ if

$$K_1 \geq K_1^* \left[1 + \left(\frac{\pi^2 K_2^2 \delta_3 + 4\delta_4 T^2}{\pi^2 K_2^2 + 4T^2} \right)^2 \right] + O(\delta_i^3) \quad (A8)$$

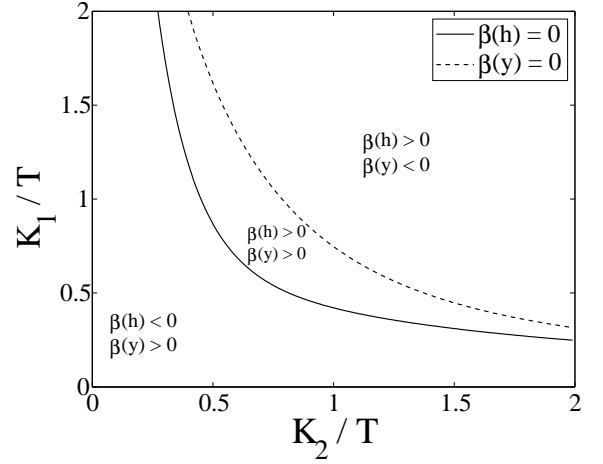


FIG. 5: The signs of $\beta(h)$ and $\beta(y)$ in the $K_1 - K_2$ plane for $K_3 = -3K_2/5$ and $K_4 = 4K_1/5$. The line which indicates $\beta(h) = 0$ always lies below the line describing $\beta(y) = 0$ and consequently h and y are never both irrelevant.

and $\beta(y) \leq 0$ if

$$\begin{aligned} K_1 \geq K_1^* \left[1 + \left(\frac{\pi^2 K_2^2 \delta_3 + 4\delta_4 T^2}{\pi^2 K_2^2 + 4T^2} \right)^2 \right. \\ \left. + 2 \left(\frac{2\pi K_2 T (\delta_4 - \delta_3)}{\pi^2 K_2^2 + 4T^2} \right)^2 \right] + O(\delta_i^3) \quad (A9) \end{aligned}$$

where $K_1^* = 4T^2/(\pi^2 K_2)$. The relative signs of $\beta(h)$ and $\beta(y)$ are shown in Fig. 5 and from Eqs. (A8) and (A9) we have calculated that the two lines describing the zeros of $\beta(h)$ and $\beta(y)$ are always separated by

$$\frac{32T^4 K_2 (\delta_4 - \delta_3)^2}{(\pi^2 K_2^2 + 4T^2)^2} > 0 \quad (A10)$$

and thus there are no values of K_1 and K_2 for small K_3 and K_4 where the 4-fold anisotropy and vortices are *both* irrelevant.

APPENDIX B: DUALITY MAPPING

This appendix will outline the derivation of Eq. (5.1).

It is useful to first consider \mathcal{F}_θ in Eq. (3.2) with $h = \eta = 0$, but to include the effect of vortices. In other words, we do wish to impose periodicity under $\theta_i \rightarrow \theta_i + 2\pi$.

First, we write the relevant portion of the action in the form

$$\frac{1}{2} \int d^2 r \partial_i \theta_a C_{ia,jb} \partial_j \theta_b \quad (B1)$$

where the indices i, j, a, b extend over x, y , and the matrix of couplings C can be easily related to the elastic constants K_i in Eq. (3.2). Now, we decouple this by a set of currents J_{ia} and write the action as

$$\int d^2 r \left[\frac{1}{2} J_{ia} C_{ia,jb}^{-1} J_{jb} + i J_{ia} \partial_i \theta_a \right] \quad (B2)$$

Imposing periodicity in $\theta_i \rightarrow \theta_i + 2\pi$ is now equivalent to the requirement that the J_{ia} are integers. We now integrate the θ_a out, and solve the resulting constraint equations by writing

$$J_{ia} = \frac{p}{2\pi} \epsilon_{ij} \partial_j \tilde{\theta}_a. \quad (\text{B3})$$

The constraints that the J_{ia} are integers can now be imposed by demanding that the $\tilde{\theta}_a$ take values which are integer multiples of $2\pi/p$. As usual, we can soften this constraint by introducing a vortex fugacity y , and so ob-

tain the effective action

$$\int d^2r \left[\frac{p^2}{8\pi^2} \epsilon_{ii'} \partial_{i'} \tilde{\theta}_a C_{ia,jb}^{-1} \epsilon_{jj'} \partial_{j'} \tilde{\theta}_b - y \sum_a \cos(p\tilde{\theta}_a) \right] \quad (\text{B4})$$

Upon explicitly working out the inverse of the matrix C , we find that this action has exactly the same form as the original \mathcal{F}_θ , with the vortex fugacity y playing the role of the lock-in field h , and the couplings K_i replaced by the couplings \tilde{K}_i in Eq. (4.9).

-
- ¹ C. Howald, H. Eisaki, N. Kaneko, M. Greven, and A. Kapitulnik, *Phys. Rev. B*, **67**, 014533 (2003).
² K. McElroy, D.-H. Lee, J. E. Hoffman, K. M. Lang, E. W. Hudson, H. Eisaki, S. Uchida, J. Lee, and J. C. Davis, *cond-mat/0404005*.
³ T. Hanaguri, C. Lupien, Y. Kohsaka, D.-H. Lee, M. Azuma, M. Takano, H. Takagi, and J. C. Davis, *Nature* **430**, 1001 (2004).
⁴ A. Fang, C. Howald, N. Kaneko, M. Greven, and A. Kapitulnik, *Phys. Rev. B* **70**, 214514 (2004).
⁵ M. Vershinin, S. Misra, S. Ono, Y. Abe, Y. Ando, and A. Yazdani, *Science* **303**, 1995 (2004).
⁶ J. M. Tranquada, H. Woo, T. G. Perring, H. Goka, G. D. Gu, G. Xu, M. Fujita, and K. Yamada, *Nature* **429**, 534 (2004).
⁷ V. Hinkov, S. Pailhes, P. Bourges, Y. Sidis, A. Ivanov, A. Kulakov, C. T. Lin, D. P. Chen, C. Bernhard, and B. Keimer, *Nature* **430**, 650 (2004).
⁸ C. Stock, W. J. L. Buyers, R. A. Cowley, P. S. Clegg, R. Coldea, C. D. Frost, R. Liang, D. Peets, D. Bonn, W. N. Hardy, and R. J. Birgeneau, *cond-mat/0408071*.
⁹ S. M. Hayden, H. A. Mook, P. Dai, T. G. Perring, and F. Dogan, *Nature* **429**, 531 (2004).
¹⁰ M. Vojta and T. Ulbricht, *Phys. Rev. Lett.* **93**, 127002 (2004).
¹¹ G. S. Uhrig, K. P. Schmidt, and M. Grüninger, *cond-mat/0402659*.
¹² M. Vojta and S. Sachdev, *cond-mat/0408461*.
¹³ D. R. Nelson and B. I. Halperin, *Phys. Rev. B* **19**, 2457 (1979).
¹⁴ A. P. Young, *Phys. Rev. B* **19**, 1855 (1979).
¹⁵ V. L. Pokrovsky and A. L. Talapov, *Phys. Rev. Lett.* **42**, 65 (1979); *Zh. Eksp. Teor. Fiz.* **78**, 269 (1980) [*Sov. Phys. JETP* **51**, 134 (1980)].
¹⁶ S. Ostlund, *Phys. Rev. B* **24**, 398 (1981).
¹⁷ S. N. Coppersmith, D. S. Fisher, B. I. Halperin, P. A. Lee, and W. F. Brinkman, *Phys. Rev. B* **25**, 349 (1982).
¹⁸ H. J. Schulz, *Phys. Rev. B* **28**, 2746 (1983).
¹⁹ F. D. M. Haldane, P. Bak, and T. Bohr, *Phys. Rev. B* **28**, 2743 (1983).
²⁰ D. A. Huse and M. E. Fisher, *Phys. Rev. B* **29**, 239 (1984).
²¹ P. M. Chaikin and T. C. Lubensky, *The Principles of Condensed Matter Physics*, Cambridge University Press, Cambridge (2000).
²² S. A. Kivelson, E. Fradkin, and V. J. Emery, *Nature* **393**, 550 (1998).
²³ J. V. José, L. P. Kadanoff, S. Kirkpatrick, and D. R. Nelson, *Phys. Rev. B* **16**, 1217 (1977).
²⁴ O. Zachar, S. A. Kivelson, and V. J. Emery, *Phys. Rev. B* **57**, 1422 (1998).
²⁵ Y. Zhang, E. Demler and S. Sachdev, *Phys. Rev. B* **66**, 094501 (2002).
²⁶ S. Sachdev, *Phys. Rev. B* **31**, 4476 (1985).